

PRACE ORYGINALNE ORIGINAL PAPERS

Scientific Review – Engineering and Environmental Sciences (2018), 27 (2), 103–113
Sci. Rev. Eng. Env. Sci. (2018), 27 (2)
Przegląd Naukowy – Inżynieria i Kształtowanie Środowiska (2018), 27 (2), 103–113
Prz. Nauk. Inż. Kszt. Środ. (2018), 27 (2)
<http://iks.pn.sggw.pl>
DOI 10.22630/PNIKS.2018.27.2.10

Barbara ŚWITAŁA¹, E. James FERN²

¹Institute of Hydro-Engineering, Polish Academy of Sciences

²Department of Civil and Environmental Engineering, University of California, Berkeley

Constitutive modelling of root-reinforced granular soils – preliminary studies

Key words: constitutive modelling, root-reinforcement, granular soil, numerical modelling

Introduction

Recently, the application of soil bio-engineering methods in various fields of science is being widely considered. This interest dedicated to alternative ecological solutions derives from the fact that these measures are generally cost effective. One of the applications of soil bio-engineering is slope stabilisation with vegetation or other organic materials.

It has been shown that the presence of vegetation on slopes and dunes improves their stability by increasing the shear strength of the soil (Preti & Giadrossich, 2009; Stokes, Atger, Bengough, Fourcaud & Sidle 2009; Rees & Ali, 2012). There are two main factors through which roots influence soil strength: mechanical root reinforcement; soil desatu-

ration, which is a direct consequence of evapotranspiration. Roots and soil form a composite which works similarly to concrete and steel; soil and concrete have compressive strength, and steel and root have tensile strength.

In recent decades, several experiments have been carried out and allowed a deeper insight into the mechanical behaviour of soil–root composite subjected to various loading conditions (Wu, 1976; Waldron & Dakessian, 1981; Operstein & Frydman 2000; Osman & Barakbah, 2000; Ghestem, Veylon, Bernard, Vanel & Stokes, 2014). Furthermore, some models have been developed, and provide a theoretical description and numerical modelling of some processes typical for the soil-root composite (Wu, 1976; Pollen & Simon, 2005; Dupuy, Gregory & Bengough, 2010; Schwarz, Lehmann & Or, 2010; Wan, Xue, & Zhao, 2011; Świtąła, Askarinejad, Wu, & Springman, 2018). However, due

to the fact that problems involving roots in the soil are complex (partial soil saturation, evapotranspiration, interactions between soil particles and roots, various external factors), better recognition and deeper understanding is required. Therefore, it is crucial to develop new paradigms, further develop existing constitutive models, and carry out additional laboratory tests on soil–root composites. Obtained information will enable more accurate modelling of the impact of vegetation on slope stability.

The research presented in this paper presents some elements of the extension of an existing constitutive model for granular soils called Nor–Sand (Jefferies, 1993) for soil–root composites. Preliminary studies focus on the model development, implementation into MATLAB and testing its sensitivity to defined values of new model parameters.

Basic assumptions of the Nor–Sand model

The Nor–Sand model is formulated in the critical state soil mechanics framework (Roscoe, Schofield & Wroth, 1958) and follows the same principles as original Cam–Clay (Roscoe & Schofield, 1963). However, Nor–Sand can be viewed as an elasto-plastic bounding surface model (Fern, 2016), which permits modelling the peak strength as a consequence of dilatancy rather than solely as a yielding point. The critical state is modelled as a nil dilatancy and nil change in dilatancy state according to following equation:

$$D = \frac{\partial D}{\partial \varepsilon_d^p} := 0 \quad (1)$$

where:

D – is the dilatancy;

$\partial \varepsilon_d^p$ – deviatoric plastic strain.

The model is characterized by two surfaces: yield surface and maximum yield surface which is the bounding surface. The critical state criterion (Eq. 1) has been divided into two components, namely $D = 0$ and $\partial D / \partial \varepsilon_d^p$, which correspond to the aforementioned yield surfaces.

The Nor–Sand model was developed from Nova’s stress–dilatancy flow rule (Nova, 1982) expressed as follows:

$$\eta' = M_\theta + (N - 1) \cdot D \quad (2)$$

in which:

N – dilatancy;

$\eta' = q / p'$ – effective stress ratio (q and p' are stress invariants, namely deviatoric and mean effective stress);

M_θ – critical state stress ratio, which is a function of the Lode’s angle θ .

For the case when $N = 0$, the above equation has the form identical to the Cam–Clay stress–dilatancy rule (Roscoe & Schofield, 1963).

Nor–Sand utilizes the concept of the state parameter (Ψ), which was proposed by Been and Jefferies (1985). The parameter allows simple identification of the current soil state with respect to the critical state according to following equation:

$$\Psi = e - e_{cs} \quad (3)$$

where:

e – void ratio;

e_{cs} – critical state void ratio.

State parameter takes negative values for dilative sands, positive for con-

tractive sands and null if the specimen is in the critical state.

The shape of the yield surface in the model is given by Equation 4 and is dependent on the value of N :

$$F = \eta' - \frac{M_\theta}{N} \left[1 + (N-1) \left(\frac{p'}{p_i} \right)^{\frac{N}{1-N}} \right] \quad (4)$$

for $N > 0$

$$F = \eta' - M_\theta \left[1 + \ln \left(\frac{p_i}{p'} \right) \right] \quad (5)$$

In Equations 4 and 5 p_i denotes the image pressure, which is an equivalent expression of the preconsolidation pressure p_c in the Cam–Clay model. The value of this variable determines the size of the yield surface and corresponds to the mean effective pressure at its summit (in the critical state, when $p' = p_i = p_{i,\max}$). This scalar variable can be used in the modelling of soil hardening or softening, depending on the changes of the state parameter (Ψ). Changes in the image pressure are dependent on the plastic deviator strain increments ($d\varepsilon_d^p$).

Nor–Sand can be seen as a bounding surface model. The bounding surface is called the maximum yield surface. The size of this surface can be assessed based on the dilatancy characteristics of the material. The size of the maximum yield surface is determined by the value of the maximum image pressure ($p_{i,\max}$). Jefferies (1993) postulated that the hardening and softening rate are proportional to the distance between actual and maximum stress state, which are defined on the yield surface and maximum yield sur-

face, respectively. Hardening or softening in Nor–Sand is dependent on the increment of the plastic deviatoric strain. This proportionality is defined by the hardening modulus (H). The hardening rule can be defined in its simplest form:

$$\frac{dp_i}{d\varepsilon_d^p} = H \cdot (p_{i,\max} - p_i) \quad (6)$$

Figure 1 illustrates the concept of the hardening and softening, which is implemented in the Nor–Sand model. The yield surface defines the boundary of the elastic region, whereas the maximum yield surface indicates the state which stress strives to achieve. Figure 1a shows the case when maximum yield surface is bigger than yield surface (i.e. $p_i < p_{i,\max}$) and we deal with the hardening. The case presented in Figure 1b corresponds to the softening and maximum yield surface smaller than actual yield surface (i.e. $p_i > p_{i,\max}$).

The maximum image pressure is dependent on the dilatancy characteristics of the given material and on the value of the parameter N and can take the following forms:

$$\frac{p_{i,\max}}{p'} = \left(1 + D_{\min} \frac{N}{M_{tc}} \right)^{\frac{N-1}{N}} \quad \text{for } N > 0 \quad (7)$$

$$\frac{p_{i,\max}}{p'} = \exp \left(-\frac{D_{\min}}{M_{tc}} \right) \quad (8)$$

where:

D_{\min} – minimum value of dilatancy;
 M_{tc} – stress ratio in triaxial compression.

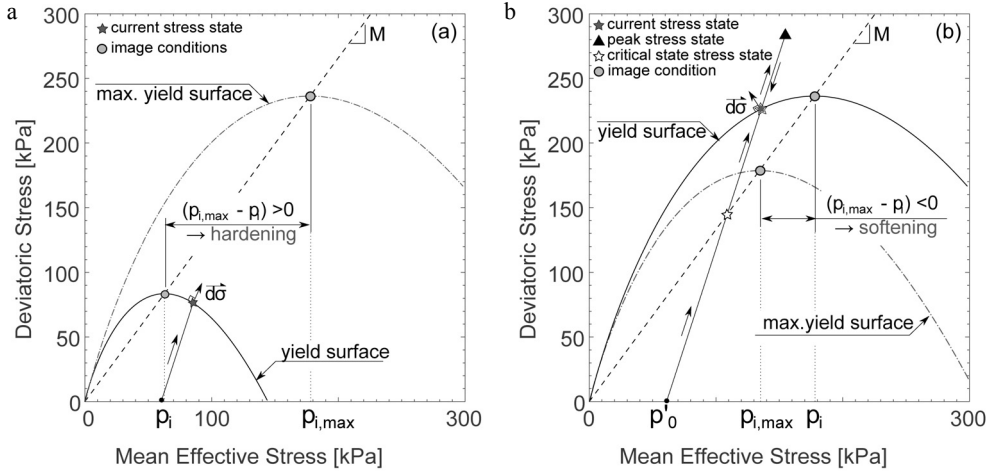


FIGURE 1. Hardening and softening concepts in the Nor–Sand model (after Fern, 2016)

Equations 7 and 8 indicate that in order to define the maximum image pressure, it is necessary to define minimum dilatancy, corresponding to the given image condition. Therefore, the image state parameter has been introduced (Ψ_i). This parameter can be explained as the state parameter (Ψ), corresponding to the given image pressure (p_i). Furthermore, the following conditions can be defined:

$$D_{\min} = \chi \frac{M_{\theta}}{M_{tc}} \psi_i \quad (9)$$

where: χ – dilatancy coefficient.

$$\psi_i = e - e_{c(p'=p_i)} \quad (10)$$

The description of a material in the elastic state is considered isotropic in the Nor–Sand model. It can be defined by two parameters, namely Poisson's ratio (ν^e) and shear modulus (G^e), which depends on the mean effective pressure. Therefore, it is also possible to define the bulk modulus (K^e).

$$G^e = A \left(\frac{p'}{p_{ref}} \right)^n \quad (11)$$

$$K^e = \frac{2(1+\nu^e)}{3(1-2\nu^e)} \cdot G^e \quad (12)$$

in which:

A – shear modulus constant;
 n – shear modulus exponent;
 p_{ref} – mean reference stress.

In conclusion, the Nor–Sand model was developed based on the main assumptions of the critical state theory. It has two yield surfaces, because of which it is possible to reflect numerically the behaviour of normally consolidated, dense sand, which, under shearing, exhibits limited compaction followed by dilation. What is important, decoupling of the two critical state conditions, given by Equation 1, is possible without the modification of the consistency condition. The incorporation of the state parameter in the model enables capturing stress–strain

characteristics of the sand with different densities and subjected to different mean effective stresses, having only one set of parameters for the considered material. The Nor–Sand model provides a solid foundation for the further development of more complex models for granular soils, such as sand–root composite.

Extension of the model for soil–root composite

The extension of the Nor–Sand model for granular soils containing roots is based on the coupled hydro-mechanical model for soil with roots (CHMR, an extension of the modified Cam–Clay) developed by Świłała (2016) and Świłała, Askarinejad, Wu and Springman (2018). In this paper, only mechanical root reinforcement is taken into consideration.

The CHMR model allows also taking into account partial saturation of the soil and the evapotranspiration phenomenon.

The modelling of the soils containing roots requires consideration of the progressive activation of the root strength, proceeding with increasing strain until the maximum strength is reached. At this moment roots start to break. Further increase of strains results in reaching the residual phase. The shear strength of the soil–root composite is presented in Figure 2.

Strains, which are responsible for the mobilisation of the soil–root composite strength are called activation strains and are defined as a sum of volumetric (ε_v) and deviatoric (ε_d) strains (Świłała et al. 2018). The increment of the activation is defined as:

$$d\varepsilon_r = d\varepsilon_v + d\varepsilon_d \quad (13)$$

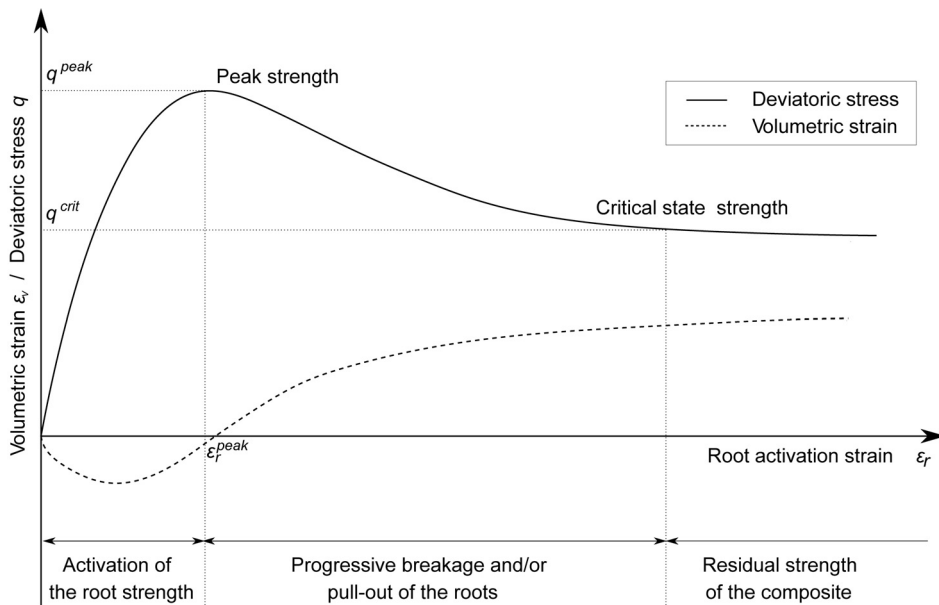


FIGURE 2. An illustration of changes in deviatoric stress and volumetric strain, depending on the level of the root activation strain (own studies)

In the extension of the Nor–Sand model for soils with mechanical root reinforcement, it is necessary to introduce additional parameters, which are dependent on the type of the plant and root content in the soil mass. These parameters allow the definition of the degree of soil–root reinforcement and, resulting from that, level of expansion of the initial and maximum yield surfaces. The description of the parameters is as follows:

– m_r^{ini} (initial root mass in the root zone) represents the fraction of the soil–root composite mass. If the characteristics of the root architecture are known, it is possible to account for changes of the root mass with depth. Furthermore, the value of m_r^{ini} governs the size of the initial yield surface (Eqs. 14 and 15).

– R_p (extended Nor–Sand constitutive parameter) defines the degree of the mechanical root reinforcement and is responsible for the size of both initial and maximum yield surfaces. The value of this parameter depends on the plant’s characteristics. The highest values are reached for the plants with the strongest roots, i.e. for trees and larger shrubs, whereas the lowest values are for grasses and herbs.

– e (void ratio) influences the level of root pull-out of the soil. If the shear deformation contributes to the soil compaction, the volume of pores decreases, causing shrinkage of the volume available for roots. As a consequence, shear strength of the composite decreases.

As it was mentioned, the impact of the mechanical root reinforcement on the soil strength is reflected in the size of the yield surface and maximum yield surface. This size is governed by the value of the image pressure and maxi-

imum image pressure, respectively. If the soil does not contain any roots, the initial value of the image pressure can be determined from the transformed Equations 4 and 5, depending on N :

$$p_{i,ini} = p' \left[\frac{1}{1-N} - \left(\frac{N}{1-N} \right) \frac{q}{p' \cdot M_\theta} \right]^{\frac{N-1}{N}}$$

for $N > 0$ (14)

$$p_{i,ini} = p' \cdot \exp \left(\frac{q}{p' \cdot M_\theta} - 1 \right)$$

for $N = 0$ (15)

The presence of the root reinforcement results in the larger initial yield surface, due to the fact that the soil–root composite has enhanced properties with respect to the bare soil. Therefore, an additional component of the image pressure can be introduced. This component governs the level of the initial enhancement and is dependent on the initial root mass of the root zone (m_r^{ini}) and on the value of the root constitutive parameter (R_p). Equations 14 and 15 are, thus, modified in a following manner according to the Equations 16 and 17:

$$p_{i,ini} = p' \left[\frac{1}{1-N} - \left(\frac{N}{1-N} \right) \frac{q}{p' \cdot M_\theta} \right]^{\frac{N-1}{N}} \cdot \exp \left(m_r^{ini} R_p \right)$$

for $N > 0$ (16)

$$p_{i,ini} = p' \cdot \exp \left(\frac{q}{p' \cdot M_\theta} - 1 \right) \cdot \exp \left(m_r^{ini} R_p \right)$$

for $N = 0$ (17)

Furthermore, mechanical root reinforcement contributes to the expansion of the maximum yield surface. The level of this expansion is dependent on the root constitutive parameter (R_p) and on the increment of the activation strains, defined by Equation 13. Involvement of the activation strain is especially important due to the fact, that enhanced strength of the soil–root composite is a function of root mobilisation, which proceeds with increasing displacement. This approach allows omitting the constant cohesion approach which is commonly used by many researchers, investigating e.g. the stability of vegetated slopes. Equations 7 and 8 have been modified to account for strength enhancement due to roots' presence:

$$p_{i,\max} = p' \left(1 + D_{\min} \frac{N}{M_{tc}} \right)^{\frac{N-1}{N}} \cdot \exp(R_p \cdot e \cdot d\varepsilon_r)$$

for $N > 0$ (18)

$$p_{i,\max} = p' \cdot \exp\left(-\frac{D_{\min}}{M_{tc}} + R_p \cdot e \cdot d\varepsilon_r\right)$$

for $N > 0$ (19)

Due to the fact that $p_{i,\max}$ appears in the Equation 6, the hardening rule is also influenced by the root reinforcement.

Sensitivity analyses

The performance of the proposed model extension has been tested, modifying a simple MATLAB code developed by Fern, Robert and Soga (2016). Laboratory tests on the sand samples

containing roots are very challenging, due to the fact that it is difficult to prepare the sample and assure that applied initial conditions will be identical in all performed tests. Moreover, plant roots are extremely heterogeneous and the shape of the root zone may evolve from one sample to another. Future work encompasses a series of triaxial compression tests on rooted sands. Then, the model validation and calibration will be possible.

The dependence of the simulation results on the different values of the model parameters (i.e. m_r^{ini} and R_p) is tested in the performed sensitivity analyses in MATLAB. The material parameters are taken from the work of Fern (2016) and are listed in the table. Drained triaxial compression tests are simulated numerically. The increment of the applied axial displacement is equal to 0.001 m.

The value of the parameter m_r^{ini} influences the size of the initial failure

TABLE. Material parameters for sensitivity analysis (Fern, 2016)

Label	Symbol	Value
Shear modulus constant	A^e	2,500 kPa
Shear modulus exponent	n^e	0.50
Poisson ratio	ν^e	0.20
Reference pressure	p_{ref}	1 kPa
Critical state effective stress ratio	M	1.33
Maximum void ratio	e_{\max}	1.00
Minimum void ratio	e_{\min}	0.54
Dilatancy parameter	N	0.30
Hardening modulus	H	200
Dilatancy coefficient	χ	2.00
Initial void ratio	e_0	0.85
Initial mean effective stress	p'_0	20 kPa

surface. In the sensitivity analysis, three different values of this parameter are considered, namely: 0.2, 0.5 and 1.0%. The results are presented in Figure 3. The graph shows, that with increasing m_r^{ini} , the elastic domain of the problem expands. The effect achieved can be compared to the preconsolidation, which is typical for cohesive soils. The specimen can sustain larger loads, resulting in the elastic response. This is an effect of the root reinforcement.

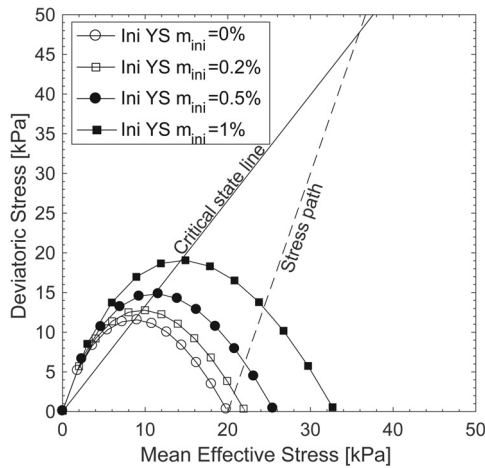


FIGURE 3. Sensitivity of the size of the initial yield surface (Ini YS) to the changes of m_r^{ini}

The influence of the root parameter is also taken into consideration, keeping the initial mass of roots constant ($m_r^{ini} = 0.5\%$). Four cases are considered, namely $R_p = 0, 20, 50$ and 80 .

Figure 4a shows the applied stress path and shapes of the yield surface and the maximum yield surface for different considered values of R_p , plotted in the p^l - q plane. The major difference is in the size of the initial yield surface, which is given by Equation 4. Similar to the previous case, the elastic domain is larger

with increasing R_p . The size of the maximum yield surface changes slightly with varying root parameter. Figure 4b presents the response of the deviatoric stress to the increasing axial strain. An interesting pattern can be observed, namely increase of the peak stress with increasing R_p . This behaviour corresponds well to the measured response of the soil-root composite, subjected to the laboratory tests (Zhang, Chen, Lin, Ji & Liu, 2010; Ghestem et al., 2014). It is expected that the reinforced soil subjected to shear is stronger, with increasing level of this reinforcement. The strength of the roots in the soil, similarly to the strength of the steel in the concrete, is being mobilised progressively and is dependent on the current level of strains. Figure 4c shows the evolution of volumetric strains during the numerical test, with advancing axial strain. When increasing root parameter, after initial compaction, negative volumetric strains which denote dilation, tend to increase. The explanation of this effect is straightforward. Single roots occupy space available in the pores between soil grains. During shearing, the available space decreases, bonds between soil particles and roots starts to break and organic material is pulled-out of the sample. The entire structure is disturbed and have a possibility to dilate progressively. The fact, that this effect can be captured numerically is significant for the further model development.

The theoretical and numerical investigations on the extension of the Nor-Sand model for soils reinforced with roots comprise preliminary studies on this problem. The model assumes the involvement of two additional parameters, which will be directly linked with various

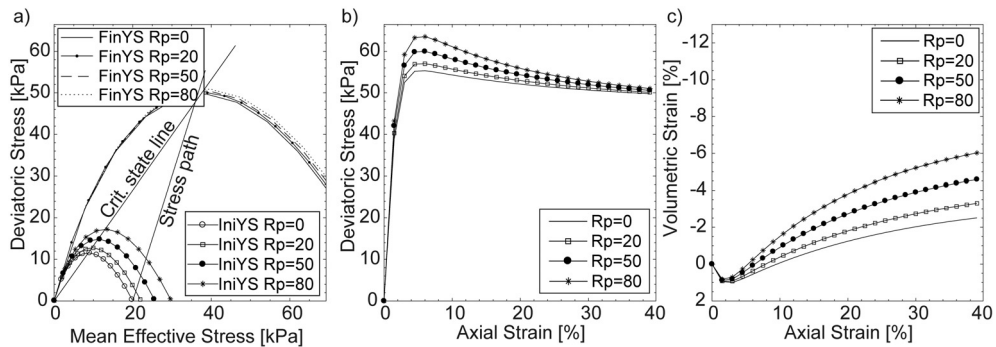


FIGURE 4. Sensitivity of the solution to the changes of R_p

root traits in the future work. The results of the sensitivity analyses are promising, the model is able to capture the behaviour of the soil–root composite subjected to shear. Modification of the initial and maximum image pressure is responsible for the expansion of the elastic domain. Moreover, the deviatoric stress, which changes with the axial strain, exhibits a larger peak and, thus, higher strength of the soil–root composite is obtained. What is important, progressive mobilisation of the roots’ strength is taken into account, assuring stepwise activation of the interactions between soil particles and roots.

Up to date, constitutive models of vegetated cohesionless soils do not exist, so there is a gap which should be filled. Therefore, presented studies provide an interesting base for the future research and further model development. Specially dedicated and designed triaxial tests will enable model verification and calibration.

The right assessment of the stability of vegetated dunes or slopes is especially significant, taking into account more conscious application of bioengineering methods in different branches of engineering (Cazzuffi, Cardile & Gioffrè, 2014).

References

- Been, K. & Jefferies, M.G. (1985). A state parameter for sands. *Géotechnique*, 35(2), 99-112. doi: 10.1680/geot.1985.35.2.99
- Cazzuffi, D., Cardile, G. & Gioffrè, D. (2014). Geosynthetic Engineering and Vegetation Growth in Soil Reinforcement Applications. *Transportation Infrastructure Geotechnology*, 1(3-4), 262-300. doi: 10.1007/s40515-014-0016-1
- Dupuy, L., Gregory, P.J. & Bengough, A.G. (2010). Root growth models: Towards a new generation of continuous approaches. *Journal of Experimental Botany*, 61(8), 2131-2143. doi: 10.1093/jxb/erp389
- Fern, J.E. (2016). *Constitutive Modelling of Unsaturated Sand and its Application to Large Deformation Modelling* (PhD thesis). Cambridge: University of Cambridge.
- Fern, J.E., Robert, D.J. & Soga, K. (2016). Modelling the stress-dilatancy relationship of unsaturated silica sand in triaxial compression tests. *Journal of Geotechnical and Geoenvironmental Engineering* 142(11). DOI: 10.1061/(ASCE)GT.1943-5606.0001546
- Ghestem, M., Veylon, G., Bernard, A., Vanel, Q. & Stokes, A. (2013). Influence of plant root system morphology and architectural traits on soil shear resistance. *Plant and Soil*, 377(1-2), 43-61. doi:10.1007/s11104-012-1572-1
- Jefferies, M.G. (1993). Nor-Sand: A simple critical state model for sand. *Géotechnique*, 43(1), 91-103.
- Nova, R. (1982). A constitutive model for soil under monotonic and cyclic loading. In *Soil*

- Mechanics – transient and cyclic loading* (pp. 343-373). Chichester: Wiley.
- Operstein, V. & Frydman, S. (2000). The influence of vegetation on soil strength. *Ground Improvement*, 4, 81-89.
- Osman, N. & Barakbah, S. (2011). The effect of plant succession on slope stability. *Ecological Engineering*, 37(2), 139-147. doi: 10.1016/j.ecoleng.2010.08.002
- Pollen, N. & Simon, A. (2005). A New Approach to Modeling the Mechanical Effects of Riparian Vegetation on Streambank Stability: A Fiber-Bundle Model. In *Impacts of Global Climate Change, World Water and Environmental Resources Congress 2005*, Anchorage, Alaska, United States. doi: 10.1061/40792(173)592
- Preti, F. & Giadrossich, F. (2009). Root reinforcement and slope bioengineering stabilization by Spanish Broom (*Spartium junceum* L.). *Hydrology and Earth System Sciences Discussions*, 6(3), 3993-4033. doi: 10.5194/hessd-6-3993-2009
- Rees, S.W. & Ali, N. (2012). Tree induced soil suction and slope stability. *Geomechanics and Geoengineering*, 7(2), 103-113. doi: 10.1080/17486025.2011.631039
- Roscoe, K.H. & Schofield, A.N. (1963). Mechanical behaviour of an idealised “wet clay”. In *Proceedings of European Conference on Soil Mechanics*, 1, 47-54.
- Roscoe, K.H., Schofield, A.N. & Wroth, C.P. (1958). On the yielding of soils. *Géotechnique*, 8, 22-53.
- Schwarz, M., Lehmann, P. & Or, D. (2010). Quantifying lateral root reinforcement in steep slopes – from a bundle of roots to tree stands. *Earth Surface Processes and Landforms*, 35(3), 354-367. doi: 10.1002/esp.1927
- Stokes, A., Atger, C., Bengough, A.G., Fourcaud, T. & Sidle, R.C. (2009). Desirable plant root traits for protecting natural and engineered slopes against landslides. *Plant and Soil*, 324(1-2), 1-30. doi: 10.1007/s11104-009-0159-y
- Świtłała, B.M. (2016). *Analysis of slope stabilisation with soil bioengineering methods* (PhD thesis). Vienna, Austria: University of Natural Resources and Life Sciences.
- Świtłała, B.M., Askarinejad, A., Wu, W. & Springman, S.M. (2018). Experimental validation of a coupled hydro-mechanical model for vegetated soil. *Géotechnique*, 68(5), 375-385. doi: 10.1680/jgeot.16.p.233
- Waldron, L.J. & Dakessian, S. (1981). Soil reinforcement by roots. *Soil Science*, 132(6), 427-435. doi: 10.1097/00010694-198112000-00007
- Wan, Y., Xue, Q. & Zhao, Y. (2011). Mechanism study and numerical simulation on vegetation affecting slope stability. *Electronic Journal of Geotechnical Engineers*, 16, 741-751.
- Wu, T.H. (1976). *Investigation of landslides on Prince of Wales Island, Alaska* (Geotechnical Report 5). Ohio: Ohio State University, Department of Civil Engineering.
- Zhang, C., Chen, L., Liu, Y., Ji, X. & Liu, X. (2010). Triaxial compression test of soil–root composites to evaluate influence of roots on soil shear strength. *Ecological Engineering*, 36(1), 19-26. doi:10.1016/j.ecoleng.2009.09.005

Summary

Constitutive modelling of root-reinforced granular soils – preliminary studies. A novel solution for the problem of modelling of soil reinforced with vegetation roots. An extension of the Nor–Sand model and its application to granular saturated or dry, soil–root composites. Model implementation in MATLAB: numerical simulations of drained triaxial compression tests, investigation of the sensitivity of the solution to different values of model parameters. Capturing the most important features of soil–root composites. Accounting for the progressive activation of the root’s strength. Indication of the ability of further model application to large-scale problems, such as slope or dune stability.

Authors' address:

Barbara Świłała
Instytut Budownictwa Wodnego PAN
80-328 Gdańsk, ul. Kościarska 7
Poland
e-mail: b.switala@ibwpan.gda.pl

Elliot James Fern
University of California, Berkeley CA
Department of Civil and Environmental
Engineering
USA
e-mail: james.fern@berkeley.edu